Environment International 109 (2017) 42–52

Contents lists available at ScienceDirect

Environment International

journal homepage: www.elsevier.com/locate/envint

The Heat Exposure Integrated Deprivation Index (HEIDI): A data-driven approach to quantifying neighborhood risk during extreme hot weather

Nikolas Krstic[a], Weiran Yuchi[a], Hung Chak Ho[b], Blake B. Walker[c], Anders J. Knudby[d], Sarah B. Henderson[a,e,*]

[a] Environmental Health Services, British Columbia Centre for Disease Control, 655 West 12th Avenue, Vancouver, BC V5Z 4R4, Canada
[b] Department of Land Surveying and Geo-informatics, Hong Kong Polytechnic University, 181 Chatham Road South, Kowloon, Hong Kong
[c] Geographisches Institut, Universität Humboldt zu Berlin, Unter den Linden 6, 10099 Berlin, Germany
[d] Department of Geography, Environment and Geomatics, University of Ottawa, 60 University Private, Ottawa, ON K1N 6N5, Canada
[e] School of Population and Public Health, University of British Columbia, 2206 East Mall, 3rd Floor, Vancouver, BC V6T 1Z3, Canada

ARTICLE INFO

Keywords:
Heat vulnerability index
Hot weather mortality
Case-crossover analysis
Spatial mapping
Index performance
Public health

ABSTRACT

Mortality attributable to extreme hot weather is a growing concern in many urban environments, and spatial heat vulnerability indexes are often used to identify areas at relatively higher and lower risk. Three indexes were developed for greater Vancouver, Canada using a pool of 20 potentially predictive variables categorized to reflect social vulnerability, population density, temperature exposure, and urban form. One variable was chosen from each category: an existing deprivation index, senior population density, apparent temperature, and road density, respectively. The three indexes were constructed from these variables using (1) unweighted, (2) weighted, and (3) data-driven Heat Exposure Integrated Deprivation Index (HEIDI) approaches. The performance of each index was assessed using mortality data from 1998–2014, and the maps were compared with respect to spatial patterns identified. The population-weighted spatial correlation between the three indexes ranged from 0.68–0.89. The HEIDI approach produced a graduated map of vulnerability, whereas the other approaches primarily identified areas of highest risk. All indexes performed best under extreme temperatures, but HEIDI was more useful at lower thresholds. Each of the indexes in isolation provides valuable information for public health protection, but combining the HEIDI approach with unweighted and weighted methods provides richer information about areas most vulnerable to heat.

1. Introduction

Extreme hot weather events are an environmental health concern of increasing importance. Although technical definitions of these events vary (Nairn et al., 2009; Robinson, 2001), they have been consistently associated with increased population morbidity (Basu and Samet, 2002; Seltenrich, 2015; Turner et al., 2012) and mortality. Under the most extreme conditions the associated mortality can be catastrophic. For example, estimates suggest that > 70,000 people died during the 2003 European heat wave event (Robine et al., 2008) and > 55,000 people died during the 2010 Russian heat wave event (Otto et al., 2012). Less dramatic mortality impacts have been documented worldwide (Åström et al., 2011; Bell et al., 2008; Coates et al., 2014; Hajat et al., 2006; Knowlton et al., 2009; Tan et al., 2007), particularly in cities where the urban heat island (UHI) effect can lead to very high exposures (Kleerekoper et al., 2012; McCarthy et al., 2010). One example occurred in greater Vancouver, Canada during the summer of 2009, which has motivated multiple studies related to hot weather epidemiology (Henderson et al., 2016; Kosatsky et al., 2012) and public health protection (Henderson and Kosatsky, 2012; Ho et al., 2017) in the region.

Extreme hot weather events are expected to increase in frequency, duration, and intensity as a result of climate change (Hayhoe et al., 2010; Meehl and Tebaldi, 2004). Because the effects are not spatially uniform, it is crucial to reliably identify areas that are at relatively higher and lower risk such that mitigation efforts can be effectively targeted. Again, this is particularly true in cities where temperatures are higher (due to the UHI), dense populations are at risk, and social vulnerabilities are spatially variable. The development and mapping of heat vulnerability indexes (HVI) is one common approach to identifying high risk areas, and these have been used to inform resource allocation and hot weather planning (Bradford et al., 2015; Reid et al., 2012).

The first step in constructing an HVI is to select the spatial variables that provide some indication of areas at higher and lower risk. While many studies have used the published literature to guide variable

* Corresponding author at: Environmental Health Services, British Columbia Centre for Disease Control, 655 West 12th Avenue, Vancouver, BC V5Z 4R4, Canada.
E-mail address: sarah.henderson@bccdc.ca (S.B. Henderson).

http://dx.doi.org/10.1016/j.envint.2017.09.011
Received 12 July 2017; Received in revised form 1 September 2017; Accepted 9 September 2017
Available online 18 September 2017

Table 1
Variables considered for inclusion in construction of the heat vulnerability indexes, falling into one of four categories. Names in brackets indicate the final variable names used in the text, reflecting modifications where necessary to ensure increasing risk of mortality with increasing variable values.

Type	Variable name (final variable name)	Modified?
Temperature exposure	Maximum air temperature (*Maximum Air Temperature*)	No
	Maximum humidex (*Maximum Humidex*)	No
	Land surface temperature (*Land Surface Temperature*)	No
Social vulnerability	Labour participation rate (*Labour Nonparticipation Rate*)	Yes
	Unemployment rate (*Unemployment Rate*)	No
	Average household income (*Average Household Income Ratio*)	Yes
	Percentage without high-school diploma (*Percentage without High School Diploma*)	No
	Percentage with a university degree (*Percentage without University Degree*)	Yes
	Home ownership percentage (*Percentage of Homes Rented*)	Yes
	Percentage of single parent families (*Percentage of Single Parent Families*)	No
	Vancouver Area Neighborhood Deprivation Index (*VANDIX*)	No
Population distribution	Population density (*Population Density*)	No
	Senior density (*Senior Density*)	No
	Children density (*Children Density*)	No
Urban form	Normalized Difference Built-up Index (*NDBI*)	No
	Normalized Difference Impervious Surface Index (*NDISI*)	No
	Normalized Difference Vegetation Index (*Negative NDVI*)	Yes
	Skyview factor (*Obstructed Sky Factor*)	Yes
	Distance to the nearest major roadway (*Inverse Distance to Nearest Major Road*)	Yes
	Major road density (*Road Density*)	No

selection (Aubrecht and Özceylan, 2013; Chow et al., 2012; Dong et al., 2014; Maier et al., 2014; Reid et al., 2009), some studies have used statistical methods to select variables from existing sets of potential predictors (Johnson et al., 2012; Loughnan et al., 2012; Wolf and McGregor, 2013). To this end, we have identified four types of variables that are relevant to the construction of an HVI. First, spatially resolved temperature maps can be used to identify urban areas that are relatively hotter, using satellite observations or models developed from remote and in-situ measurements (Hondula et al., 2012; Kershaw and Millward, 2012). Second, multiple indicators of social vulnerability have been associated with hot weather mortality in previous studies (Harlan et al., 2006; Patz et al., 2000). Third, some sensitive populations such as children and the elderly struggle to thermoregulate under extreme heat conditions (Buscail et al., 2012; Kovats and Hajat, 2008; Reid et al., 2009). Finally, highly urban areas with limited vegetation and complex impermeable and reflective materials may be particularly susceptible, beyond what is indicated by temperature mapping (Dong et al., 2014; Gabriel and Endlicher, 2011). Once variables have been selected, the HVI is typically generated through either the unweighted or weighted approaches.

The unweighted approach assumes that each variable is equally predictive of hot weather risk, so the variables are simply standardized and summed to create the HVI (Aubrecht and Özceylan, 2013; Bao et al., 2015; Chow et al., 2012; Dong et al., 2014; Wisconsin Department of Health Services, 2014). The weighted approach assumes that different variables are more or less predictive of hot weather risk, which makes HVI construction more complex. Multiple approaches to weighting have been used (El-Zein and Tonmoy, 2015; Loughnan et al., 2012; Rinner et al., 2010; Wolf and McGregor, 2013), but the most common approach is principal component analysis (PCA). In brief, scores from retained principal components are weighted by their respective variance explained. Each spatial unit is given a weighted score from each principal component, and these scores are aggregated to produce the HVI (Wolf and McGregor, 2013; Zhu et al., 2014).

Some studies have justified using the unweighted approach because the literature has not identified a single variable with a higher impact on heat vulnerability than other variables (Aubrecht and Özceylan, 2013; Wisconsin Department of Health Services, 2014). However, newer studies suggest that demographic or socioeconomic variables may play a larger role in heat vulnerability and should be given more weight (Jones et al., 2015; Linares et al., 2014). Although assigned weights can account for these differences, it makes index construction more complex and may introduce subjectivity during variable reduction and weighting analyses. Here we propose a purely data-driven approach to select and weight HVI variables and create a Heat Exposure Integrated Deprivation Index (HEIDI) based on previous work to spatially delineate temperature-mortality relationships in greater Vancouver (Ho et al., 2017). The objectives are to: (1) apply the data-driven approach to select and weight variables for inclusion in the HVI from each of four categories reflecting temperature exposure, social vulnerability, population distribution, and urban form; (2) assess and evaluate HEIDI compared with conventional unweighted and weighted approaches; and (3) identify areas of high risk for future public health protection and heat adaptation strategies.

2. Methods

2.1. Study area

Greater Vancouver is a rapidly growing urban area in the province of British Columbia, Canada. (Aubrecht and Özceylan, 2013; Wisconsin Department of Health Services, 2014). In 2016 it had a population of approximately 2.4 million residents covering an area of 2882 km^2 (Statistics Canada, 2017b). The metropolitan region comprises 21 municipalities, mostly in the Fraser River delta and surrounding foothills of the coastal mountains. The region is bounded to the north and east by mountains, to the west by the Pacific Ocean, and to the south by its border with the United States. These geographic attributes create complex microclimatic environments that can result in strong urban heat island effects on hot summer days (Ho et al., 2016).

2.2. Data sources

2.2.1. Vital statistics

The BC Vital Statistics Agency provides the BC Centre for Disease Control with daily mortality data to support its public health surveillance and protection programs. The dataset used in these analyses included all deaths within greater Vancouver from 1998 through 2014. The following information was available for each death: date of death; age in years; sex; location of death (home, hospital, residential institution, or other); underlying cause of death coded according to the 10th revision of the International Classification of Diseases (ICD-10); and the 6-digit residential postal code. All deaths attributed to transport accidents (ICD-10 codes V01-V99) were removed. The residential 6-

digit postal codes were geolocated using the Canadian Postal Code Conversion File, and values for the 20 spatial variables described below (Table 1) were extracted to the coordinates.

2.2.2. Three spatial variables reflecting temperature exposure

Temperature exposures in greater Vancouver can vary within tens of meters (Tsin et al., 2016), and we included three spatial variables to characterize this on hot summer days: land surface temperature; air temperature; and humidex (Table 1). Humidex is an estimate of apparent temperature used in Canada, produced from a combination of air temperature and relative humidity (Masterton and Richardson, 1979). Previous publications describe the development, evaluation, and application of these maps for greater Vancouver (Aminipouri et al., 2016; Ho et al., 2014; Ho et al., 2017; Ho et al., 2016; Tsin et al., 2016). In brief, we used combinations of Landsat 5 Thematic Mapper (TM) and Landsat 7 Enhanced Thematic Mapper (ETM +) images taken on cloud-free summer days when the maximum air temperature was ≥ 25 °C at Vancouver International Airport (YVR). The land surface temperature map was derived from standard methods (Barsi et al., 2003; Coll et al., 2010) using Landsat 5 TM data only. The maximum daily air temperature and Humidex maps were derived from random forest models associating temperatures observed at 59 local weather stations with land surface temperature, normalized difference water index (NDWI) (Gao, 1996), skyview factor (Hodul et al., 2016), elevation, and solar radiation (Ho et al., 2014; Ho et al., 2016). The skyview factor describes the proportion of the sky that is obscured at any given location, with values of 0 and 1 representing an entirely obstructed and unobstructed sky, respectively (Oke, 1988).

2.2.3. Eight spatial variables reflecting social vulnerability

Many different variables can be used to describe social and/or material deprivation within a population and these variables are often combined into single indexes, using methods similar to those already described (Liberatos et al., 1988; Messer et al., 2006). The Vancouver Area Neighborhood Deprivation Index (VANDIX) is a weighted index derived from variables measured in the Canadian census and their perceived effect on population health in the study area. In brief, a survey was distributed among local medical health officers asking them to rank the importance of 21 different variables with respect to their association with poor health outcomes in greater Vancouver (Bell and Hayes, 2012). The seven variables with the highest aggregate scores were selected and used to create the VANDIX, which can be mapped at the level of census dissemination area (DA). These DAs typically contain populations between 400 and 700 (Statistics Canada, 2017a). Any missing VANDIX values were replaced with the average of the VANDIX values from bordering DAs, weighted by the length of the shared perimeter.

In addition to including VANDIX in the pool of potential HVI variables, we also included each of its seven contributing variables, in case any one of them was more predictive of hot weather risk than the combination of all. These variables are: labour participation rate; unemployment rate; average household income; percentage of the population without a high school diploma; percentage of the population with a university degree; percentage of homes owned; and percentage of single-parent families (Table 1). Some of the variables were modified prior to analysis so that increasing values were associated with increasing hot weather risk. The final variables included the labour nonparticipation rate, the percentage of the population without a university degree, the percentage of homes rented, and the average household income ratio. The latter was taken as the inverse of the average household income multiplied by the minimum value.

2.2.4. Three spatial variables reflecting population distribution

Variables reflecting the distributions of the entire population, young children (≤ 10 years), and seniors (≥ 65 years) were included in the analyses (Table 1). Population data from the 2006 Canadian census were extracted from SimplyMap (Geographic Research, 2016) at the DA level in a polygon format. The area of each DA was calculated in ArcGIS 10.3 (Environmental Systems Research Institute, 2014). The population densities were calculated by dividing the total population, the number of young children, and the number of seniors by the DA areas. A raster with a resolution of 60 m was then created for each of the three density variables.

2.2.5. Six spatial variables reflecting urban form

Although the temperature exposure maps capture some variability in urban form, we included six other variables that may have important and independent relationships with hot weather risk (Table 1). The skyview factor data used in the temperature exposure maps were considered independently because areas with highly obstructed skies may be more vulnerable due to the delayed escape of long-wave radiation and the effects on air currents (Gál et al., 2009). These data were generated for greater Vancouver from Landsat 5 TM images (Hodul et al., 2016), and were expressed as the proportion of obstructed sky to ensure increasing risk with increasing variable values. Other urban form variables derived from remote sensing data were the Normalized Difference Built-up Index (NDBI) (Zha et al., 2003), Normalized Difference Impervious Surface Index (NDISI) (Xu, 2010), and Normalized Difference Vegetation Index (NDVI). All three variables take values between −1 and 1, with larger values generally characterizing areas that are developed, contain impervious surfaces, or contain vegetation, respectively. These variables were derived from the same Landsat 5 TM images used to create the land surface temperature map (Ho et al., 2014). The NDVI was multiplied by −1 so that larger values indicated less vegetated areas, because increased vegetation is associated with decreased hot weather risk (Jenerette et al., 2007).

Finally, we included variables indicating the presence and density of major roads. This decision was based on preliminary analyses indicating increased hot weather mortality risk in areas with higher nitrogen oxide (NO) concentrations as modelled by land use regression (Henderson et al., 2007; M. Wang et al., 2013). To better understand the preliminary finding we repeated analyses with all variables in the NO model: length of major roads within 100 m; length of major roads within 1000 m; population density within 2500 m; elevation; latitude; and longitude. Of these, we found that the length of major roads within 100 m was more strongly associated with hot weather mortality than estimated NO concentrations. This makes sense, given that roads have relatively high storage heat flux, meaning the net uptake and release of heat (R. Wang et al., 2013; Xu et al., 2008). Road network data were taken from the DMTI Spatial CanMap 2013 data (DMTI Spatial Inc., 2013), and spatial variables were created for distance to the nearest major road and for density of major roads within a 100 m radius. The distance variable was modified by taking the inverse so that larger values corresponded with increased risk.

2.3. Data-driven delineation of high risk areas

Values for each of the 20 spatial variables were extracted to the coordinates of the residential 6-digit postal codes for each death in the mortality dataset. The shape of the temperature-mortality relationship for each variable was characterized using the case-crossover approach we have described in detail elsewhere (Ho et al., 2017). In brief, Humidex observations from the Environment Canada weather station at YVR were used as the time-varying measure of exposure in a time-stratified design. Every decedent was assigned daily mean Humidex values for the day of death (case day) and for all occurrences of the same weekday within the same calendar month (control days). The mortality data were then subset to those individuals who had a case day or a control day within the 99.9th percentile of the YVR observations from 1998 to 2014. As such, the analytic dataset included only deaths that occurred either on an extremely hot day or a comparable cooler day.

Conditional logistic regression was used to assess which of the spatial variables showed increasing risk of hot weather mortality associated with increasing variable values. The binary response variable was 1 for case days and 0 for control days, conditioned on a unique identifier for the individual decedents. The only explanatory term in the model was an interaction between daily mean Humidex at YVR and a binary variable indicating whether the residence of each decedent was located in an area above or below some threshold value of the spatial variable. For example, if the threshold value of *VANDIX* was 3.0, all decedents who lived in areas of equal or higher deprivation would have a value of 1 for the indicator variable while others would have a value of 0. For each of the 20 spatial variables we tried 100 threshold values equally spaced between the 1st and 99th percentiles, resulting in a total of 2000 regressions. The odds ratio (OR) for the above-threshold group was extracted from each model, and the 100 ORs for each spatial variable were plotted against their respective threshold values. Finally, a locally weighted smoother (LOESS) was fit to each scatter plot and the shape of the LOESS was assessed for deviation from the baseline OR, calculated using all deaths in the analytic dataset. We refer to these fitted smoothers as the "threshold-OR" curves from herein.

2.4. Spatial variable selection for index construction

We selected one variable from each of the four categories to use in construction of the indexes. This decision was made to ensure that the indexes were both parsimonious and easy to interpret. Based on the threshold-OR curves described above, we needed criteria by which to select one spatial variable from each of the four categories: temperature exposure; social vulnerability; population distribution; and urban form. The selection criteria considered (1) the variable correlations within categories and between categories, (2) the threshold-OR inflection point, (3) the threshold-OR slope above the inflection point, and (4) the area under the threshold-OR curve (AUC). A variable was considered to be a good candidate if it was not highly correlated with other candidate variables and the threshold-OR curve had an early point of inflection, a steep slope, and/or a high AUC. If a candidate variable best satisfied the last three criteria, but was highly correlated to the other variables selected for the index, it was potentially omitted in favour of another candidate variable (within the same category) that was less correlated to the other selected variables.

The inflection point indicates the threshold value of the spatial variable at which the threshold-OR curve becomes consistently higher than the baseline OR. To systematically identify the inflection point, approximate second derivatives of the threshold-OR curves were computed for each threshold value and then ranked from largest to smallest. Starting from the value with the largest second derivative, we proceeded sequentially, assigning the inflection point to the first value that satisfied two conditions: (1) the slopes before and after this point were positive, and (2) the OR at that point was smaller than the ORs at the points with the next three largest second derivatives. These criteria ensured that we did not select a threshold value in the middle of the incline. Variables with early inflection points were favoured because they were often associated with high AUC values and larger ORs at the extreme variable values. Any variable with a flat threshold-OR curve was automatically removed from consideration.

After the inflection point had been identified, the slope of the relationship above the inflection point was assessed using linear regression. This criterion was important because the magnitude of the slope indicated the speed with which the temperature-mortality relationship could change. As such, steeper slopes were favoured during spatial variable selection. Finally, the AUC of the threshold-OR curve was calculated using the baseline OR as the lower boundary, the inflection point as the leftmost boundary, and the end of the curve as the rightmost boundary. Large AUC values suggested that the inflection point occurred early in the range of variable values or that the slope was large. The AUC also reflects the presence of any peaks or valleys in the threshold-OR curve, which would not be characterized by the inflection point and slope criteria alone.

2.5. Index construction

2.5.1. Conventional approaches

The unweighted approach used the summation of the four selected spatial variables, under the assumption that each variable had the same impact on heat vulnerability. Variables were standardized using z-score transformation, such that each variable had a mean of 0 and a standard deviation of 1. The result was a linear sum of the transformed variables (Eq. (1)). The weighted approach was similar, but assumed that each of the selected variables had a different impact on vulnerability. The individual weights were determined by the slope of the temperature-morality relationship above the inflection point, scaled so that the sum of all four weights was 1. The weighted values of each Z-score standardized variable were then summed together to create the index (Eq. (2)).

$$HVI_{unweighed} = Z_1 + Z_2 + Z_3 + Z_4 \quad (1)$$

$$HVI_{slope\text{-}weighed} = A*Z_1 + B*Z_2 + C*Z_3 + D*Z_4 \quad (2)$$

2.5.2. The Heat Exposure Integrated Deprivation Index (HEIDI) approach

The HEIDI approach is a novel method that we propose to be an effective alternative or supplement to conventional approaches. This purely data-driven technique takes the spatial sum of OR maps created for each index variable, based on the results of spatial delineation analyses described above. For example, if the highest threshold value for *VANDIX* was 5.0 and it produced an above-threshold OR of 1.20, all areas of greater Vancouver with equal or greater deprivation would be assigned a value of 1.20. If the second-highest threshold value for *VANDIX* was 4.8 and it produced an above-threshold value of 1.18, all areas with deprivation between 4.8 and 5.0 would be assigned a value of 1.18, and so on, essentially creating an isopleth for each of the 100 threshold values (illustrated in Fig. 1). Once the OR map had been generated for each spatial variable in the index, the raster values were summed to generate a map of the HEIDI values.

2.6. Index assessment

The unweighted, weighted, and HEIDI indexes were each rescaled from their 1st and 99th percentile values to produce values between 0 and 5. Maps of the indexes were then generated at a 60 m resolution, and index values were extracted to the residential locations of each decedent in the mortality dataset. The case-crossover analyses were repeated with 100 threshold values for each of the indexes, and the resulting threshold-OR curves were used to evaluate the performance of each index and to identify areas of low, moderate, and high heat vulnerability on each index map. Specifically, we mapped areas where each index indicated ORs < 1.1, between 1.1 and 1.2, and > 1.2, and compared the maps. We expected to see increasing hot weather risk with increasing values of each index, and maximum ORs greater than those for any of the four contributing variables.

Recall that the data were originally subset to individuals who had a case day or a control day within the 99.9th percentile of observations at YVR, which was 24 °C. We also tested the performance of the indexes by repeating the same case-crossover and threshold-OR curve analyses for mortality datasets subset to less extreme temperatures, ranging from 20 to 23 °C. Here we expected to see weaker relationships degrading towards the baseline as the temperature cut-off was reduced, but slower degradation would indicate improved utility for defining areas of higher heat vulnerability. Finally, all postal codes within greater Vancouver were geolocated and index values were extracted to these points so that population-weighted correlations between the indexes could be calculated. We chose not to calculate simple spatial

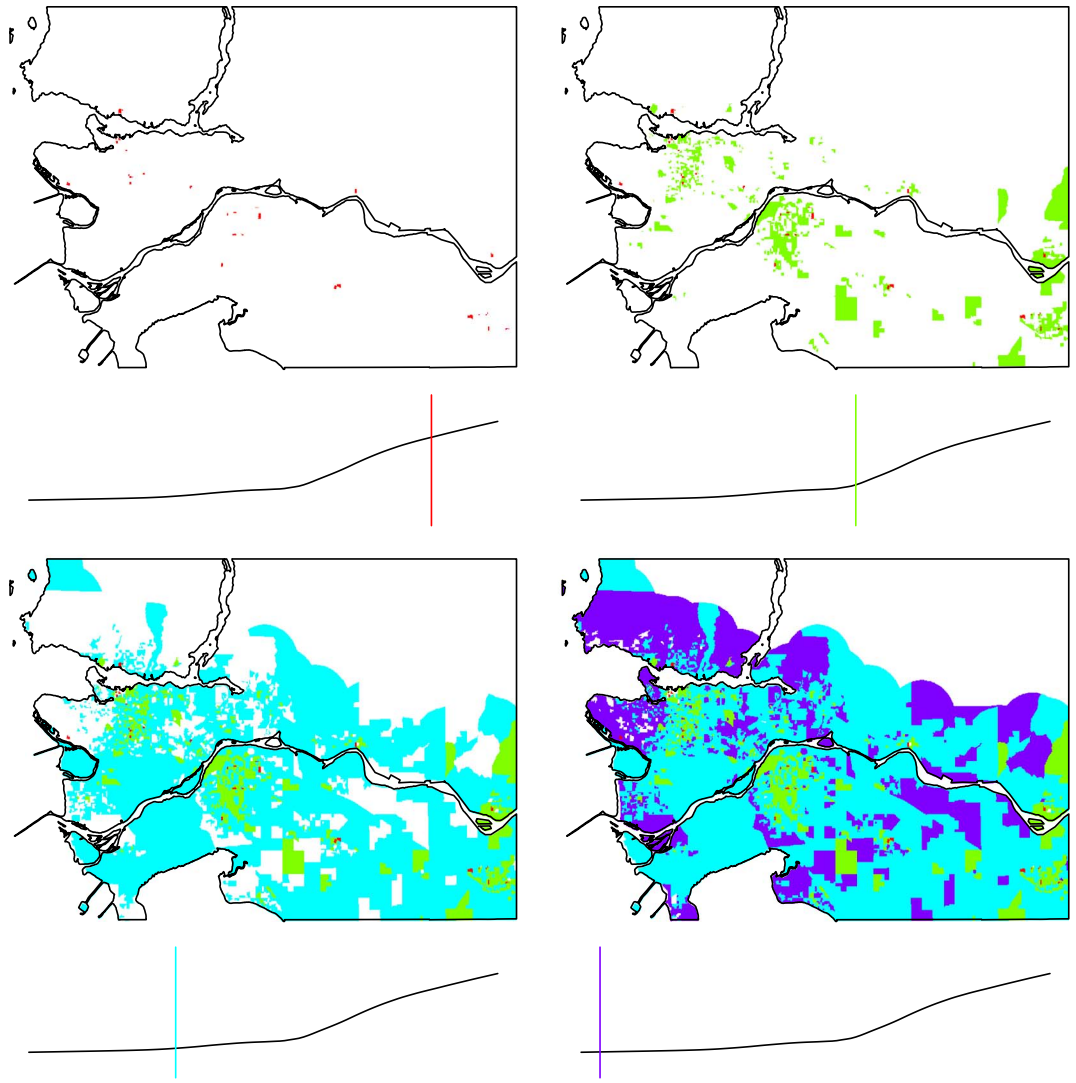

Fig. 1. An illustrative example of the odds ratio (OR) isopleth maps generated for each of the variables included in the Heat Exposure Integrated Deprivation Index (HEIDI). Using multiple threshold values for each variable (4 shown here, 100 used in the analyses), areas that were equal to or exceeded each value were assigned the corresponding OR from the threshold-OR curve shown. This was done sequentially from the largest threshold value to the smallest value.

correlations because greater Vancouver has mountainous areas and a large agricultural land reserve that are thinly populated.

3. Results and discussion

3.1. Summary of the mortality data used for evaluation

The mortality dataset used in most of the analysis was based on the 99.9th percentile of temperature observations at YVR, and it included a total of 1006 deaths. Of these, 272 of the deaths occurred on six extremely hot days and the remaining 734 deaths occurred on a cooler day, but had a control day that was extremely hot. On extremely hot days the mortality counts ranged from 27 to 67 while on cooler days they ranged from 14 to 48. The baseline OR [95% confidence interval] for these deaths was 1.03 [1.02, 1.05], meaning that a 1-degree increase in mean daily Humidex at YVR was associated with a 3.4% [1.8%, 5.0%] increase in the odds of mortality among this subset. When the temperature cut-off was dropped from 24 °C to 20 °C the number of deaths in the subset was increased to 33,032, but the overall effect of a 1-degree increase in mean daily Humidex at YVR remained stable at 1.02 [1.02, 1.03].

One limitation of vital statistics data is that they consistently fail to identify decedents for whom temperature caused or contributed to the death. The criteria for this certification are rarely met, so it is challenging to separate expected deaths from excess deaths during extreme hot weather events (Henderson et al., 2016). To address this limitation we restricted the main analytic dataset to deaths that occurred on extremely hot days and comparable cooler days, thereby increasing the proportion of deaths that would have been excess due to heat rather than expected under typical conditions. The same approach was taken in the antecedent work (Ho et al., 2017), though here we provide more information about impacts of the temperature cut-off with respect to the analytic dataset (Table 2) and the performance of the HVI. Other approaches could be taken. For example, Ho et al. (2017) reported that the performance was improved by restricting the analytic dataset to decedents who died at home or in the community, rather than in care.

Another way to strengthen the results could be more algorithmic consideration of the lagged effects of high temperatures on population health. For example, time series analyses in the study region have shown that mortality is best modelled using the 2-day average of maximum temperatures (Henderson and Kosatsky, 2012; Henderson et al., 2013). Here we consider only the effect of same-day temperature on mortality using the case-crossover design, meaning that we do not necessarily capture the effect of an extremely hot day on mortality the

Table 2
Summary statistics for the analytic mortality datasets generated using different threshold temperatures to define extremely hot days, including average values of the index variables. The 24 °C data were used to generate the heat vulnerability indexes.

		Temperature cut-off				
		24 °C	23 °C	22 °C	21 °C	20 °C
Number of extremely hot days included		6	20	41	100	203
Deaths included		1006	3423	6826	16,513	33,032
Deaths on extremely hot days		272	839	1785	4450	11,105
Deaths on comparable cooler days		734	2584	5041	12,063	21,927
Mean humidex (°C)	Hot days	33.0	32.9	32.9	32.9	32.9
	Cooler days	32.7	32.9	32.9	32.9	32.9
VANDIX	Hot days	0.03	− 0.05	− 0.04	− 0.04	− 0.04
	Cooler days	− 0.10	− 0.06	− 0.05	− 0.05	− 0.05
Mean senior density (persons/km^2)	Hot days	1152	1100	1103	1106	1141
	Cooler days	1042	1090	1115	1112	1117
Mean road density (m/km^2)	Hot days	3720	3485	3417	3463	3322
	Cooler days	3191	3295	3293	3274	3278

following day. However, the six extremely hot days included in main analyses (Table 2) were clustered into three hot periods: July 27–28, 1998; July 22, 2006; and July 28–30, 2009. When the threshold temperature was dropped from 24 °C to 22 °C, these clusters were extended to: July 26–29, 1998; July 21–23, 2006; and July 26–31, 2009. Focusing on specific hot periods rather than including all individual hot days might help future studies using similar methods to better capture the lagged effects of extreme heat.

3.2. Variables selected for index construction

The threshold-OR plots for the 20 spatial variables showed different relationships with increasing variable values (Fig. 2), from decreasing mortality risk (e.g. *Population Density*) to flat (e.g. *Percentage without University Degree*) to increasing risk across the entire range (e.g. *Road Density*). Our objective was to select one variable from each of the four categories, applying the correlation, inflection point, slope, and AUC criteria. In the temperature exposure category, *Maximum Humidex* had a sharp inflection and steep slope compared with *Land Surface Temperature* and *Maximum Air Temperature*. This finding was also reported in previous work (Ho et al., 2017), and thus the *Maximum Humidex* variable was chosen for inclusion in the HVI.

Of the population distribution variables only *Senior Density* had a clear inflection point, and it was chosen for inclusion in the HVI. All variables in the social vulnerability category showed some increase in mortality risk across the range of values, with the exception of *Percentage without University Degree*. The *Labour Nonparticipation Rate* variable showed the strongest relationship with risk, followed by the *VANDIX* composite. This result has also been reported elsewhere (Ho et al., 2017), but here we chose to include the *VANDIX* because both the *Senior Density* and the *Labour Nonparticipation Rate* variables capture the retired population and have a relatively high correlation (r = 0.30). Conversely, the correlation between *VANDIX* and *Senior Density* was low (r = 0.05). Finally, many of the urban form variables had midpoint inflections along with moderate slopes. However, the *Road Density* variable was chosen for the HVI because of its higher AUC and lower correlations with the other chosen variables.

The range of correlations between the four chosen variables was 0.03–0.45, where most correlations were < 0.06 and the strongest correlation was between *VANDIX* and *Maximum Humidex*. This relatively high correlation likely reflects the fact that the least deprived areas of greater Vancouver are closer to the ocean and have a lot of vegetation compared with the most deprived areas. We retained both variables because they measure fundamentally different constructs. *Road Density* and *Senior Density* were both heavily right-skewed because of the presence of extremely large density values at some locations. The variable weights for the weighted index were taken as the slope above the inflection point in the threshold-OR plots. These were 0.419 for *Maximum Humidex*, 0.270 for *VANDIX*, 0.229 for *Road Density*, and 0.081 for *Senior Density*. Slopes were used instead of other plot parameters because they best reflect how quickly heat vulnerability escalates as a variable increases.

Variables similar to the ones used to create the HVIs have been employed in previous studies to either develop heat indexes or identify areas of heat vulnerability. Humidex has been used to generate hourly prediction maps of potential heat stress for the Greater Toronto Area in Canada (Kershaw and Millward, 2012). Although the authors created a very practical tool for public health organizations, they do not integrate other social parameters that may influence heat vulnerability. Other socioeconomic status indexes similar to VANDIX have also been used to map risk. In France, the FDep99 social deprivation index (Rey et al., 2009b) and a heat exposure index were combined to examine how their interaction affected the number of heat-related mortalities (Rey et al., 2009a). The authors reported that excess mortality within the fifth deprivation quintile was approximately double excess mortality within the first deprivation quintile for areas of Paris in the top three quintiles of heat exposure.

Previous work on seniors has reported that they are among the most vulnerable subpopulations during extreme hot weather (Borrell et al., 2006; Gabriel and Endlicher, 2011; Kenny et al., 2010), though we have found that younger seniors are at higher risk in greater Vancouver (Kosatsky et al., 2012). One concern about the inclusion of senior density within an HVI is that it becomes difficult to determine which populations are at risk in a given area. The index may show that an area is highly vulnerable because it has a dense population of seniors, or because of other factors that put the whole population at risk. Finally, road network variables have been used in other studies to investigate heat vulnerability and urban heat island effects (Chen et al., 2012; Inostroza et al., 2016). Road density had a strong positive correlation with nocturnal land surface temperature in Shenzhen, China but minor importance within the HVI constructed for Santiago, Chile. There are multiple methods to calculate the road density, but we found the 100 m buffer useful for clearly identifying and visualizing local differences.

3.3. Index comparisons

The mean (standard deviation) index values of all postal codes for the unweighted, weighted, and HEIDI indexes were 0.95 (0.58), 1.74 (0.82), 0.75 (0.77), respectively (Table 3). Upon extracting the index values to each of the geolocated postal codes, the correlation between the indexes were as follows: unweighted index and weighted index was 0.89; unweighted index and HEIDI was 0.69; and weighted index and HEIDI was 0.77. The spatial correlations between HEIDI and the other indexes may be moderate for different reasons. First, we opted to calculate the correlations for postal codes rather than all cells in the index maps to avoid inflating the correlation values because of the abundance of low vulnerability areas with very low population sizes. Second, many of the pre-inflection ORs for the contributing variables were near the baseline value (Fig. 2) meaning that the majority of postal codes had HEIDI values between 0 and 1 (Table 3).

3.4. Index performance

The threshold-OR plots for the unweighted, weighted, and HEIDI indexes showed different risk profiles over the range of values from 0 to 5, with maximum OR values of 1.25, 1.30, and 1.23, respectively (Fig. 3). The unweighted and weighted approaches had inflection points occurring at approximately 1.5 and 2.5, respectively, but the weighted index had a steeper slope beyond the inflection. In contrast, the threshold-OR curve for HEIDI was constantly increasing across all values. For the unweighted, weighted, and HEIDI approaches the approximate ranges of variation in the threshold-OR curves were from

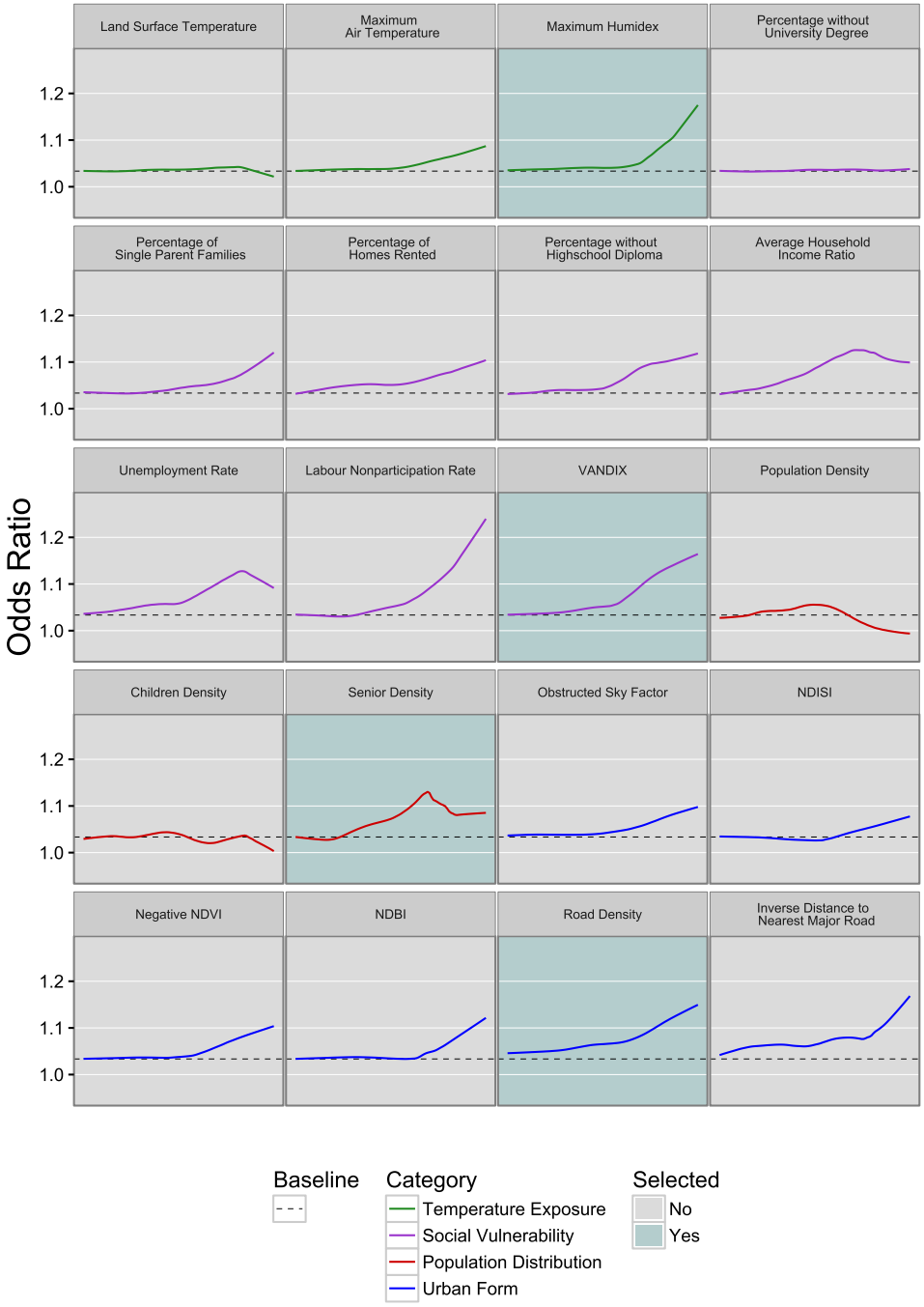

Fig. 2. Plots showing the variable threshold values compared with their associated odds ratios (OR) for the 20 potential index variables, separated into four categories. The threshold-OR curves were fitted using a locally weighted smoother (LOESS). The black dotted line in each plot is the baseline OR (1.03). The variables with a light cyan background were selected for inclusion in the three different heat vulnerability indexes.

Table 3
Summary statistics for the heat vulnerability indexes, including the percentages of postal codes within each of the index intervals.

Index intervals	Indexes		
	Unweighted index	Weighted index	HEIDI
0–1	61.3%	17.4%	80.2%
> 1–2	34.3%	46.6%	11.7%
> 2–3	3.5%	29.4%	5.3%
> 3–4	0.6%	5.7%	2.0%
> 4–5	0.3%	0.8%	0.8%
Index mean	0.95	1.74	0.75
Index SD	0.58	0.82	0.77

1.5–5, 2.5–5, and 0–5, respectively (Fig. 3), making it meaningless to compare index values. Instead, we converted index values to estimated ORs for every postal code and mapped areas of low, moderate, and high risk for each using ORs < 1.1, between 1.1 and 1.2, and > 1.2, respectively. The resulting maps show considerable spatial variation between the approaches. The unweighted index had very small areas within the moderate and high risk zones (0.9% of postal codes), while these areas were larger in the weighted (3.1% of postal codes) and HEIDI (9.7% of postal codes) indexes (Fig. 3).

All three indexes indicate areas of increased risk in some of the same locations: the downtown eastside of the City of Vancouver; urban areas of the Burnaby municipality; small areas of the New Westminster municipality; and the easternmost municipality of Abbotsford. Moderate and high risk areas according to the unweighted index were small and sparse, whereas the weighted and HEIDI indexes showed larger areas

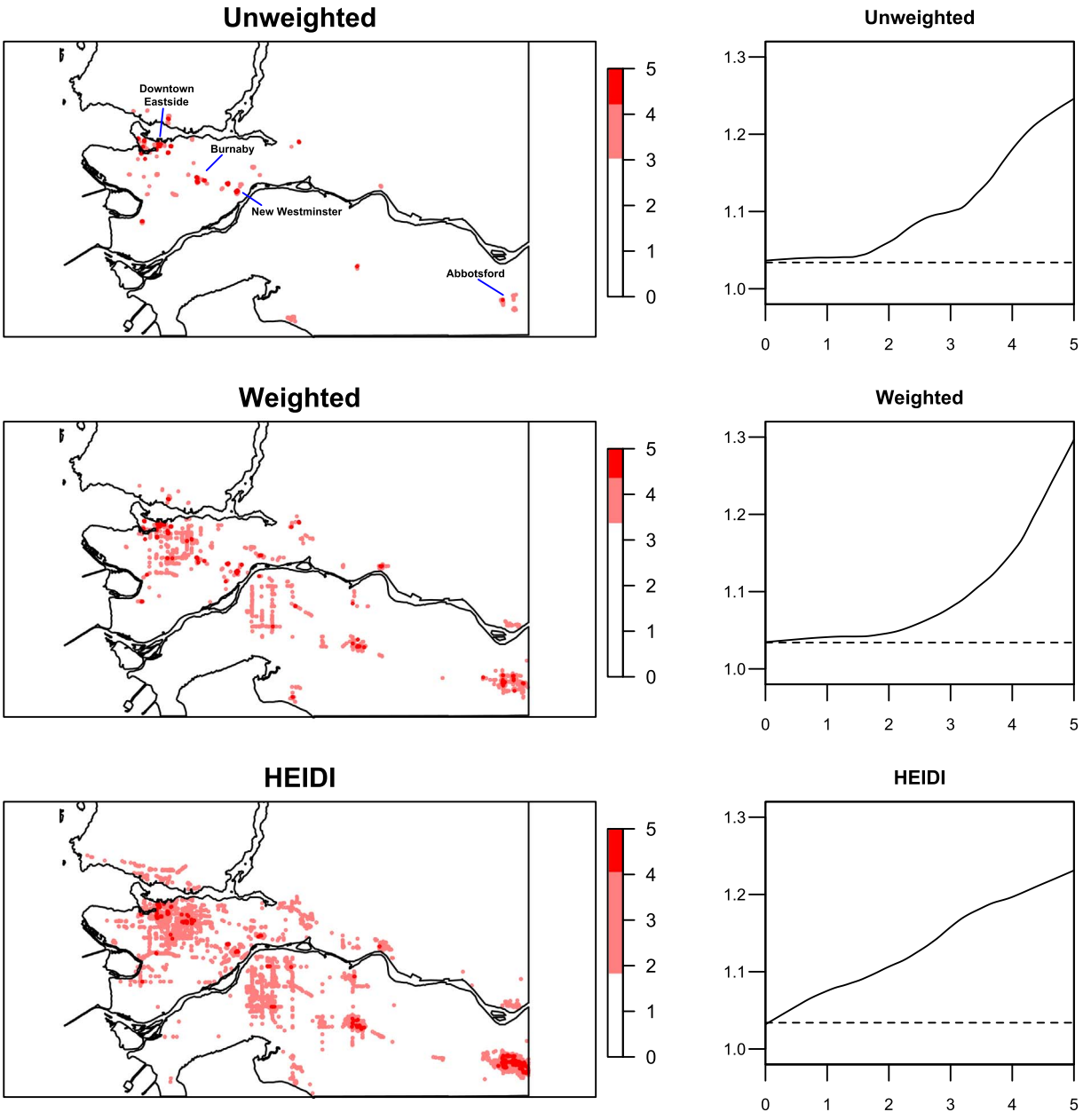

Fig. 3. Odds ratio (OR) maps of the indexes based on the threshold-OR curves for each index. White areas indicate OR values < 1.1 (< 10% increase in risk on a hot day), pink dots indicate postal codes with OR values between 1.1 and 1.2 (10–20% increase in risk), and red dots indicate postal codes with OR values > 1.2 (> 20% increase in risk). The black dashed line on the threshold-OR plots indicates the baseline risk (OR = 1.03). (For interpretation of the references to color in this figure legend, the reader is referred to the web version of this article.)

with more continuity, and both highlighted the impact of the road density variable. Overall, HEIDI indicated some general areas of heat vulnerability throughout the developed areas of each municipality in greater Vancouver, and particularly highlighted the downtown eastside in the city of Vancouver and the entire city of Abbotsford (Fig. 3). The identification of these larger, more comprehensive areas is a function of the linear increase in risk observed across all HEIDI values.

When the definition of an extremely hot day was varied to generate different subsets of the mortality data (Table 2), we found that all three indexes showed some increase in risk at all temperature thresholds (Fig. 4). In general, the patterns of the threshold-OR curves observed at a 24 °C persisted down to 20 °C, but were attenuated at each temperature reduction. However, the inflection points for the unweighted and weighted indexes increased as the temperature threshold decreased while risk across HEIDI values remained linear. Overall it appears that each index remains informative at less extreme temperatures, but that the distribution of risk is most consistent across HEIDI values.

Other studies have also evaluated their HVIs using mortality data. An HVI constructed for London, England (Wolf and McGregor, 2013) was assessed by how well it could predict high mortality and ambulance dispatches during heat wave events (Wolf et al., 2014). Different assessment approaches were used, including computation of prediction skill scores and quasi-Poisson regression to assess changes in relative risk. Although predictive performance of the HVI was not strong, the results supported its potential as an indicator of areas where above average morbidity and mortality could be expected. Another HVI created for metropolitan areas across the United States (Reid et al., 2009) was evaluated to verify whether it identified areas with increased morbidity and mortality during exceptionally hot days (Reid et al., 2012). Hospitalization and mortality counts for five states were

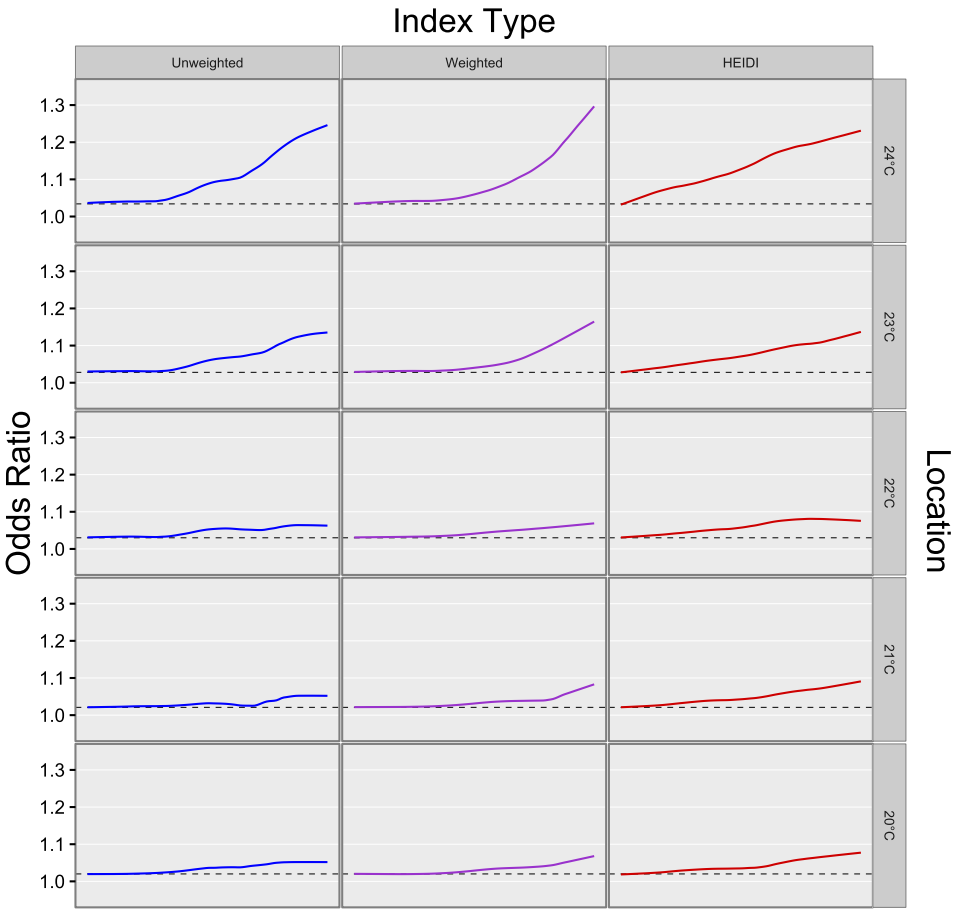

Fig. 4. The three indexes were created based on odds ratios (OR) calculated with mortality data from extremely hot days, defined as mean temperature > 24 °C at Vancouver International Airport (top row). Other plots show the threshold-OR curves for each index at less restrictive definitions of extremely hot days, from > 20 °C to > 23 °C. The black dashed line on the threshold-OR plots indicates the baseline risk (OR = 1.03).

regressed against the interaction of the HVI and a custom heat exposure metric representing hot days. The results demonstrated that the HVI primarily classified areas of general health vulnerability, but could potentially be capable of identifying increased risks of heat-related illnesses on exceptionally hot days. We found that HEIDI performed well against the mortality data using the threshold-OR approach, with high index values suggesting high risk and moderate index values suggesting moderate risk. Further, we found that areas of risk identified by HEIDI were consistent with those identified by more conventional approaches, but that HEIDI indicated a larger population at risk.

We believe that the strength of the HEIDI approach lies in this linear increase in the threshold-OR curve across the index values. An unweighted index constructed with four spatial variables can only take high values in areas where values for each of the contributing variables are high. The underlying assumption is that risk of mortality is multiplicatively higher in areas where all variables are high compared with areas where only one variable is high. As such, areas that might be at high risk due to a single variable cannot take a high index value, and the information is lost. The situation is similar for the weighted approach, but the index can take high values under broader conditions, depending on the variable weights. On the other hand, an index constructed using data-driven maps of mortality risk can take a high value at any location where the OR for any contributing variable is high, better reflecting the independent and combined risks of the variable set.

One result of the greater linearity observed using the HEIDI approach is that larger areas (and therefore larger populations) are identified as being at moderate risk. This raises the question of how information from HEIDI can be used for risk communication and population protection when compared with approaches that focus on more spatially constrained areas. Since the extreme hot weather event of 2009 (Kosatsky et al., 2012), the regional health authorities in greater Vancouver have developed heat health emergency plans for targeting interventions at high-risk populations during future events. These plans include visiting all residential care facilities to assess indoor temperatures, contacting socially isolated individuals, and distributing resources such as drinking water and cooling fountains to some specific locations. Unfortunately, these types of interventions are too resource-intensive to be extended to populations at moderate risk. However, there are other interventions that can help to protect the population and that do not incur the same costs. Some examples include identifying large, air-conditioned buildings that could be used as public cooling shelters, or asking public swimming pools to reduce their rates and/or extend their hours during extreme heat. Tools such as HEIDI can help to identify the neighborhoods in which such simple interventions could have the largest potential impacts. This is particularly true for urban areas such as greater Vancouver, where extreme heat is an emerging threat rather than an established pattern. Even so, cities with hotter climates still show spatial variability in the mortality impacts of locally extreme temperatures (Harlan et al., 2013), and the methods we propose should be replicable in any urban area where individual-level mortality data are available at high spatial resolution. In areas without such data we recommend that HVIs be constructed by methods that are more Boolean than arithmetic, such that the index can take a high value in any area where any contributing variable is high. As with HEIDI, this will allow for better characterization of areas with moderate risk, which may have much larger populations than the spatially constrained areas at highest risk.

Conflicts of interest

None.

Funding sources

This research did not receive any specific grant from funding agencies in the public, commercial, or not-for-profit sectors. Open access publication was supported by Health Canada.

Acknowledgements

Thanks to our peer reviewers who helped to strengthen this work.

References

Aminipouri, M., Knudby, A., Ho, H.C., 2016. Using multiple disparate data sources to map heat vulnerability: Vancouver case study. Can. Geogr. 60, 356–368.
Åström, D.O., Bertil, F., Joacim, R., 2011. Heat wave impact on morbidity and mortality in the elderly population: a review of recent studies. Maturitas 69, 99–105.
Aubrecht, C., Özceylan, D., 2013. Identification of heat risk patterns in the US National Capital Region by integrating heat stress and related vulnerability. Environ. Int. 56, 65–77.
Bao, J., Li, X., Yu, C., 2015. The construction and validation of the heat vulnerability index, a review. Int. J. Environ. Res. Public Health 12, 7220–7234.
Barsi, J.A., Barker, J.L., Schott, J.R., 2003. An atmospheric correction parameter calculator for a single thermal band earth-sensing instrument. In: Proceedings of the Geoscience and Remote Sensing Symposium: 2003 IGARSS'03 Proceedings 2003 IEEE International.
Basu, R., Samet, J.M., 2002. Relation between elevated ambient temperature and mortality: a review of the epidemiologic evidence. Epidemiol. Rev. 24, 190–202.
Bell, N., Hayes, M., 2012. The vancouver area neighbourhood deprivation index (VANDIX): a census-based tool for assessing small-area variations in health status. Can. J. Public Health 103, S28–S32.
Bell, M.L., O'Neill, M.S., Ranjit, N., Borja-Aburto, V.H., Cifuentes, L.A., Gouveia, N.C., 2008. Vulnerability to heat-related mortality in Latin America: a case-crossover study in Sao Paulo, Brazil, Santiago, Chile and Mexico City, Mexico. Int. J. Epidemiol. 37, 796–804.
Borrell, C., Marí-Dell'Olmo, M., Rodríguez-Sanz, M., Garcia-Olalla, P., Caylà, J.A., Benach, J., Muntaner, C., 2006. Socioeconomic position and excess mortality during the heat wave of 2003 in Barcelona. Eur. J. Epidemiol. 21, 633–640.
Bradford, K., Abrahams, L., Hegglin, M., Klima, K., 2015. A heat vulnerability index and adaptation solutions for Pittsburgh, Pennsylvania. Environ. Sci. Technol. 49, 11303–11311.
Buscail, C., Upegui, E., Viel, J.-F., 2012. Mapping heatwave health risk at the community level for public health action. Int. J. Health Geogr. 11, 38.
Chen, Z., Gong, C., Wu, J., Yu, S., 2012. The influence of socioeconomic and topographics factors on nocturnal urban heat islands: a case study in Shenzhen, China. Int. J. Remote Sens. 33, 3834–3849.
Chow, W.T., Chuang, W.-C., Gober, P., 2012. Vulnerability to extreme heat in metropolitan Phoenix: spatial, temporal, and demographic dimensions. Prof. Geogr. 64, 286–302.
Coates, L., Haynes, K., O'Brien, J., McAneney, J., de Oliveira, F.D., 2014. Exploring 167 years of vulnerability: an examination of extreme heat events in Australia 1844–2010. Environ. Sci. Pol. 42, 33–44.
Coll, C., Galve, J.M., Sanchez, J.M., Caselles, V., 2010. Validation of Landsat-7/ETM + thermal-band calibration and atmospheric correction with ground-based measurements. IEEE Trans. Geosci. Remote Sens. 48, 547–555.
DMTI Spatial Inc., 2013. DMTI CanMap Streetfiles. Markham, Ontario.
Dong, W., Liu, Z., Zhang, L., Tang, Q., Liao, H., Li, X.E., 2014. Assessing heat health risk for sustainability in Beijing's urban heat island. Sustainability 6, 7334–7357.
El-Zein, A., Tonmoy, F.N., 2015. Assessment of vulnerability to climate change using a multi-criteria outranking approach with application to heat stress in Sydney. Ecol. Indic. 48, 207–217.
Environmental Systems Research Institute, 2014. ArcGIS Desktop: Release 10.3. Environmental Systems Research Institute, Redlands, CA, USA.
Gabriel, K.M.A., Endlicher, W.R., 2011. Urban and rural mortality rates during heat waves in Berlin and Brandenburg, Germany. Environ. Pollut. 159, 2044–2050.
Gál, T., Lindberg, F., Unger, J., 2009. Computing continuous sky view factors using 3D urban raster and vector databases: comparison and application to urban climate. Theor. Appl. Climatol. 95, 111–123.
Gao, B.C., 1996. NDWI - a normalized difference water index for remote sensing of vegetation liquid water from space. Remote Sens. Environ. 58, 257–266.
Geographic Research, 2016. Census 2006.
Hajat, S., Armstrong, B., Baccini, M., Biggeri, A., Bisanti, L., Russo, A., Paldy, A., Menne, B., Kosatsky, T., 2006. Impact of high temperatures on mortality: is there an added heat wave effect? Epidemiology 17, 632–638.
Harlan, S.L., Brazel, A.J., Prashad, L., Stefanov, W.L., Larsen, L., 2006. Neighborhood microclimates and vulnerability to heat stress. Soc. Sci. Med. 63, 2847–2863.
Harlan, S.L., Declet-Barreto, J.H., Stefanov, W.L., Petitti, D.B., 2013. Neighborhood effects on heat deaths: social and environmental predictors of vulnerability in Maricopa County, Arizona. Environ. Health Perspect. 121, 197.
Hayhoe, K., Sheridan, S., Kalkstein, L., Greene, S., 2010. Climate change, heat waves, and mortality projections for Chicago. J. Great Lakes Res. 36, 65–73.
Henderson, S.B., Kosatsky, T., 2012. A data-driven approach to setting trigger temperatures for heat health emergencies. Can. J. Public Health 227–230.
Henderson, S.B., Beckerman, B., Jerrett, M., Brauer, M., 2007. Application of land use regression to estimate long-term concentrations of traffic-related nitrogen oxides and fine particulate matter. Environ. Sci. Technol. 41, 2242–2248.
Henderson, S.B., Wan, V., Kosatsky, T., 2013. Differences in heat-related mortality across four ecological regions with diverse urban, rural, and remote populations in British Columbia, Canada. Health Place 23, 48–53.
Henderson, S.B., Gauld, J.S., Rauch, S.A., McLean, K.E., Krstic, N., Hondula, D.M., Kosatsky, T., 2016. A proposed case-control framework to probabilistically classify individual deaths as expected or excess during extreme hot weather events. Environ. Health 15.
Ho, H.C., Knudby, A., Sirovyak, P., Xu, Y.M., Hodul, M., Henderson, S.B., 2014. Mapping maximum urban air temperature on hot summer days. Remote Sens. Environ. 154, 38–45.
Ho, H.C., Knudby, A., Xu, Y., Hodul, M., Aminipouri, M., 2016. A comparison of urban heat islands mapped using skin temperature, air temperature, and apparent temperature (Humidex), for the greater Vancouver area. Sci. Total Environ. 544, 929–938.
Ho, H.C., Knudby, A., Walker, B.B., Henderson, S.B., 2017. Delineation of spatial variability in the temperature-mortality relationship on extremely hot days in greater Vancouver, Canada. Environ. Health Perspect. 125.
Hodul, M., Knudby, A., Ho, H.C., 2016. Estimation of continuous urban sky view factor from Landsat data using shadow detection. Remote Sens. 8.
Hondula, D.M., Davis, R.E., Leisten, M.J., Saha, M.V., Veazey, L.M., Wegner, C.R., 2012. Fine-scale spatial variability of heat related mortality in Philadelphia County, USA, from 1983–2008: a case-series analysis. Environ. Health 11.
Inostroza, L., Palme, M., de la Barrera, F., 2016. A heat vulnerability index: spatial patterns of exposure, sensitivity and adaptive capacity for Santiago de Chile. PLoS One 11.
Jenerette, G.D., Harlan, S.L., Brazel, A., Jones, N., Larsen, L., Stefanov, W.L., 2007. Regional relationships between surface temperature, vegetation, and human settlement in a rapidly urbanizing ecosystem. Landsc. Ecol. 22, 353–365.
Johnson, D.P., Stanforth, A., Lulla, V., Luber, G., 2012. Developing an applied extreme heat vulnerability index utilizing socioeconomic and environmental data. Appl. Geogr. 35, 23–31.
Jones, B., O'Neill, B.C., McDaniel, L., McGinnis, S., Mearns, L.O., Tebaldi, C., 2015. Future population exposure to US heat extremes. Nat. Clim. Chang. 5, 652–655.
Kenny, G., Yardley, J., Brown, C., Sigal, R.J., Jay, O., 2010. Heat stress in older individuals and patients with common chronic diseases. CMAJ 182, 1053–1060.
Kershaw, S.E., Millward, A.A., 2012. A spatio-temporal index for heat vulnerability assessment. Environ. Monit. Assess. 184, 7329–7342.
Kleerekoper, L., van Esch, M., Salcedo, T.B., 2012. How to make a city climate-proof, addressing the urban heat island effect. Resour. Conserv. Recycl. 64, 30–38.
Knowlton, K., Rotkin-Ellman, M., King, G., Margolis, H.G., Smith, D., Solomon, G., Trent, R., English, P., 2009. The 2006 California heat wave: impacts on hospitalizations and emergency department visits. Environ. Health Perspect. 117, 61.
Kosatsky, T., Henderson, S.B., Pollock, S.L., 2012. Shifts in mortality during a hot weather event in Vancouver, British Columbia: rapid assessment with case-only analysis. Am. J. Public Health 102, 2367–2371.
Kovats, R.S., Hajat, S., 2008. Heat stress and public health: a critical review. Annu. Rev. Public Health 29, 41–55.
Liberatos, P., Link, B.G., Kelsey, J.L., 1988. The measurement of social class in epidemiology. Epidemiol. Rev. 10, 87–121.
Linares, C., Mirón, I.J., Montero, J.C., Criado-Álvarez, J.J., Tobías, A., Díaz, J., 2014. The time trend temperature–mortality as a factor of uncertainty analysis of impacts of future heat waves. Environ. Health Perspect. 122, A118.
Loughnan, M., Nicholls, N., Tapper, N.J., 2012. Mapping heat health risks in urban areas. Int. J. Popul. Res. 2012.
Maier, G., Grundstein, A., Jang, W., Li, C., Naeher, L.P., Shepherd, M., 2014. Assessing the performance of a vulnerability index during oppressive heat across Georgia, United States. Weather Clim. Soc. 6, 253–263.
Masterton, J., Richardson, F., 1979. Humidex: A Method of Quantifying Human Discomfort Due to Excessive Heat and Humidity Ed˙Eds. Downsview, Ontario, Canada, Environment Canada, Atmospheric Environment.
McCarthy, M.P., Best, M.J., Betts, R.A., 2010. Climate change in cities due to global warming and urban effects. Geophys. Res. Lett. 37.
Meehl, G.A., Tebaldi, C., 2004. More intense, more frequent, and longer lasting heat waves in the 21st century. Science 305, 994–997.
Messer, L.C., Laraia, B.A., Kaufman, J.S., Eyster, J., Holzman, C., Culhane, J., Elo, I., Burke, J.G., O'Campo, P., 2006. The development of a standardized neighborhood deprivation index. J. Urban Health 83, 1041–1062.
Nairn, J., Fawcett, R., Ray, D., 2009. Defining and predicting excessive heat events, a national system. In: Modelling and Understanding High Impact Weather: Extended Abstracted of the Third CAWCR Modelling Workshop.
Oke, T.R., 1988. Street design and urban canopy layer climate. Energ. Buildings 11, 103–113.
Otto, F.E., Massey, N., Oldenborgh, G., Jones, R., Allen, M., 2012. Reconciling two approaches to attribution of the 2010 Russian heat wave. Geophys. Res. Lett. 39.
Patz, J.A., McGeehin, M.A., Bernard, S.M., Ebi, K.L., Epstein, P.R., Grambsch, A., Gubler, D.J., Reiter, P., Romieu, I., Rose, J.B., Samet, J.M., Trtanj, J., 2000. The potential health impacts of climate variability and change for the United States: executive summary of the report of the health sector of the U.S. National Assessment. Environ. Health Perspect. 108, 367–376.
Reid, C.E., O'Neill, M.S., Gronlund, C.J., Brines, S.J., Brown, D.G., Diez-Roux, A.V., Schwartz, J., 2009. Mapping community determinants of heat vulnerability. Environ. Health Perspect. 117, 1730.
Reid, C.E., Mann, J.K., Alfasso, R., English, P.B., King, G.C., Lincoln, R.A., Margolis, H.G.,

Rubado, D.J., Sabato, J.E., West, N.L., 2012. Evaluation of a heat vulnerability index on abnormally hot days: an environmental public health tracking study. Environ. Health Perspect. 120, 715.
Rey, G., Fouillet, A., Bessemoulin, P., Frayssinet, P., Dufour, A., Jougla, E., Hémon, D., 2009a. Heat exposure and socio-economic vulnerability as synergistic factors in heat-wave-related mortality. Eur. J. Epidemiol. 24.
Rey, G., Jougla, E., Fouillet, A., Hemon, D., 2009b. Ecological association between a deprivation index and mortality in France over the period 1997–2001: variations with spatial scale, degree of urbanicity, age, gender and cause of death. BMC Public Health 9.
Rinner, C., Patychuk, D., Bassil, K., Nasr, S., Gower, S., Campbell, M., 2010. The role of maps in neighborhood-level heat vulnerability assessment for the city of Toronto. Cartogr. Geogr. Inf. Sci. 37, 31–44.
Robine, J.-M., Cheung, S.L.K., Le Roy, S., Van Oyen, H., Griffiths, C., Michel, J.-P., Herrmann, F.R., 2008. Death toll exceeded 70,000 in Europe during the summer of 2003. C. R. Biol. 331, 171–178.
Robinson, P.J., 2001. On the definition of a heat wave. J. Appl. Meteorol. 40, 762–775.
Seltenrich, N., 2015. Between extremes: health effects of heat and cold. Environ. Health Perspect. 123, A275.
Statistics Canada, 2017a. Dissemintation Area (DA) Definition. Dictionary, Census of Population, 2016: Statistics Canada.
Statistics Canada, 2017b. Population and Dwelling Count Highlight Tables, 2016 Census.
Tan, J., Zheng, Y., Song, G., Kalkstein, L.S., Kalkstein, A.J., Tang, X., 2007. Heat wave impacts on mortality in Shanghai, 1998 and 2003. Int. J. Biometeorol. 51, 193–200.
Tsin, P.K., Knudby, A., Krayenhoff, E.S., Ho, H.C., Brauer, M., Henderson, S.B., 2016. Microscale mobile monitoring of urban air temperature. Urban Clim. 18, 58–72.
Turner, L.R., Barnett, A.G., Connell, D., Tong, S., 2012. Ambient temperature and cardiorespiratory morbidity: a systematic review and meta-analysis. Epidemiology 23, 594–606.
Wang, R., Henderson, S.B., Sbihi, H., Allen, R.W., Brauer, M., 2013. Temporal stability of land use regression models for traffic-related air pollution. Atmos. Environ. 64, 312–319.
Wang, M., Yan, X., Liu, J., Zhang, X., 2013. The contribution of urbanization to recent extreme heat events and a potential mitigation strategy in the Beijing-Tianjin-Hebei metropolitan area. Theor. Appl. Climatol. 114, 407–416.
Wisconsin Department of Health Services, 2014. Wisconsin Heat Vulnerability Index.
Wolf, T., McGregor, G., 2013. The development of a heat wave vulnerability index for London, United Kingdom. Weather Clim. Extrem. 1, 59–68.
Wolf, T., McGregor, G., Analitis, A., 2014. Performance assessment of a heat wave vulnerability index for Greater London, United Kingdom. Weather Clim. Soc. 6, 32–46.
Xu, H., 2010. Analysis of impervious surface and its impact on urban heat environment using the Normalized Difference Impervious Surface Index (NDISI). Photogramm. Eng. Remote Sens. 76, 557–565.
Xu, W., Wooster, M.J., Grimmond, C.S.B., 2008. Modelling of urban sensible heat flux at multiple spatial scales: a demonstration using airborne hyperspectral imagery of Shanghai and a temperature-emissivity separation approach. Remote Sens. Environ. 112, 3493–3510.
Zha, Y., Gao, J., Ni, S., 2003. Use of normalized difference built-up index in automatically mapping urban areas from TM imagery. Int. J. Remote Sens. 24, 583–594.
Zhu, Q., Liu, T., Lin, H., Xiao, J., Luo, Y., Zeng, W., Zeng, S., Wei, Y., Chu, C., Baum, S., 2014. The spatial distribution of health vulnerability to heat waves in Guangdong Province, China. Glob. Health Action 7.